

Regular article

An ab initio study of electrophilic aromatic substitution*

Daniel Zerong Wang, Andrew Streitwieser

Department of Chemistry, University of California, Berkeley, CA 94720-1460, USA

Received: 11 June 1998 / Accepted: 3 September 1998 / Published online: 23 February 1999

Abstract. Proton affinities are calculated at all reactive positions for the normal benzenoid hydrocarbons, benzene, naphthalene, phenanthrene and anthracene, a strained benzenoid hydrocarbon, biphenylene, and a nonalternant hydrocarbon, fluoranthene, and the results are compared to experimental protodetritiation rates. Methods used include PM3 and Hartree-Fock calculations at the STO-3G, 3-21G*, 6-31G* and MP2//6-31G* levels. Generally good agreement is found between theory and experiment with 6-31G* giving the best correlations.

Key words: Proton affinity – Protodetritiation – Protonation – Orientation – Alternant hydrocarbon

Polycyclic aromatic hydrocarbons (PAHs) have received increasing recent interest because of their ubiquitous environmental pollution, and because of carcinogenesis and mutagenesis [1, 2]. There is increasing evidence that carcinogenic/mutagenic activity which ultimately leads to PAH-DNA adduct formation is initiated by electrophilic and/or oxidation chemistry involving PAH carbocations or radical cations [3–7]. Protonated PAHs have long been known in solution and have been characterized, in particular, by NMR [4]. A number of protonated PAHs are also known in the gas phase and have provided the corresponding proton affinities. Protonated PAHs are also valuable models for interpreting electrophilic aromatic substitution [8]. Calculations of the corresponding π -molecular orbital (MO) systems provided early successes for the Hückel MO (HMO) method (“localization” energies) [8] in qualitative and quantitative applications to aromatic substitution. Approximation of these localization energies was the earliest application of Fukui’s frontier electron approach [9, 10], an approach that is also related to Dewar’s perturbation theory of aromatic substitution [11–13]. A number of theoretical approaches within the π -approx-

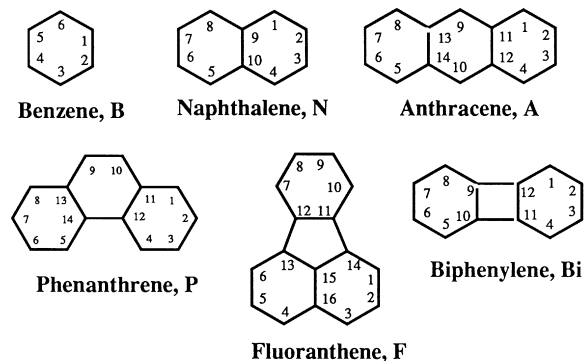
imation have been suggested for quantitative correlations of electrophilic aromatic substitution but for benzenoid PAHs they are all mutually related and give similar correlations [8]. For other types of PAH, however, these HMO-based methods as well as a number of semiempirical MO approaches fail. For example, none of the methods give good correlations for the reactivity of different positions in fluoranthene [14, 15]. Similarly, although all HMO-based methods predict the β -position of biphenylene to be more reactive than the α -position, in contrast to naphthalene, the magnitude of the orientation specificity is incorrect [16]. It seems clear that in many of these cases ring-strain effects play a role that is not accounted for by semiempirical π -electron methods. The purpose of this paper is to test whether ab initio methods can give a satisfactory account of models for aromatic substitution. The methods are applied to several normal benzenoid PAHs, an alternant but strained benzenoid PAH (biphenylene), and a nonalternant PAH, fluoranthene.

We chose to calculate the protonated PAHs because this would provide proton affinities (PAs) that could be compared with experimental values [17]; however, these PA values pertain only to the most stable protonated compound corresponding to the most reactive position, but they still serve to calibrate the calculations. Moreover, it has long been known that the rates of many electrophilic aromatic substitution reactions correlate well with equilibrium values for protonation in solution [8]. In particular, rates for protodetritiation are available for many positions on PAHs [15, 18, 19] and provide appropriate experimental data for testing with theory. The ab initio computations employed the Gaussian 92 and Gaussian 94 computer programs [20]. The structures of benzene, naphthalene, anthracene, phenanthrene, fluoranthene, biphenylene and their protonated carbocations were fully optimized at the HF/STO-3G, HF/3-21G* and HF/6-31G* levels with single-point calculations at the MP2/6-31G*//HF6-31G* level. The PAHs themselves have been optimized at the HF/6-31G* level previously [21], but the results are repeated here for convenience. Semiempirical calculations are available for many of the protonated derivatives [4, 22]. Total

* Contribution to the Kenichi Fukui Memorial Issue
Correspondence to: A. Streitwieser

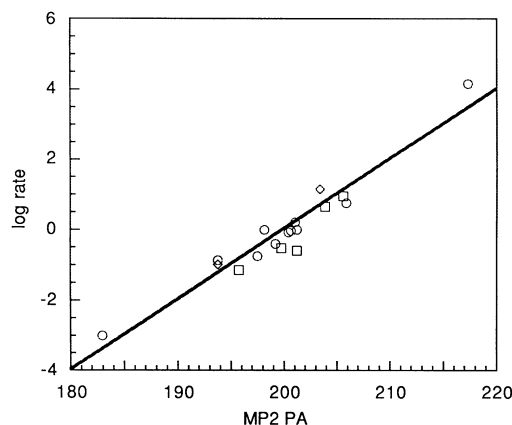
Table 1. The total electronic energies (hartree) calculated by PM3, HF/STO-3G, HF/3-21G*, HF/6-31G* and MP2//HF/6-31G* methods

Molecule	PM3 ^a	HF/STO-3G	HF/3-21G*	HF/6-31G*	MP2/6-31G*//HF/6-31G*
Benzene ^b	0.037232	-227.89136	-229.41945	-230.70314	-231.45659
Benzene-1	0.338458	-228.26258	-229.72218	231.01468	-231.74813
Naphthalene ^b	0.064577	-378.68685	-381.21581	-383.35505	-384.61185
Naphthalene-1	0.347288	-379.08675	-381.54283	-383.69034	-384.92764
Naphthalene-2	0.352542	-379.07896	-381.53548	-383.68433	-384.92065
Phenanthrene ^b	0.087351	-529.48745	-533.01572	-536.00976	-537.77200
Phenanthrene-1	0.366374	-529.89137	-533.34464	-536.34758	-538.09180
Phenanthrene-2	0.370586	-529.88538	-533.33953	-536.34399	-538.08676
Phenanthrene-3	0.368387	-529.88949	-533.34293	-536.34718	-538.08945
Phenanthrene-4	0.370644	-529.88877	-533.34323	-536.34646	-538.09137
Phenanthrene-9	0.365962	-529.89276	-533.34625	-536.34941	-538.09239
Anthracene ^b	0.097926	-529.47248	-533.00347	-535.99877	-537.76087
Anthracene-1	0.370914	-529.88760	-533.34299	-536.34688	-538.08897
Anthracene-2	0.377221	-529.87913	-533.33549	-536.34103	-538.08153
Anthracene-9	0.357713	-529.90840	-533.36211	-536.36428	-538.10717
Biphenylene ^{b,c}	0.174737	-453.41759	-456.43787	-459.01459	-460.52364
Biphenylene-1 ^c	0.462910	-453.81098	-456.75514	-459.34383	-460.83247
Biphenylene-2 ^c	0.455292	-453.82763	-456.77224	-459.36229	-460.84779
Fluoranthene	0.127118	-604.30325	-608.32163	-611.74562	-613.76097
Fluoranthene-1	0.406105	-604.70907	-608.65052	-612.08474	-614.07932
Fluoranthene-2	0.411821	-604.69911	-608.64263	-612.07689	-614.07295
Fluoranthene-3	0.400043	-604.71961	-608.66085	-612.09488	-614.08859
Fluoranthene-7	0.406662	-604.70468	-608.64783	-612.08138	-614.08162
Fluoranthene-8	0.403426	-604.71161	-608.65466	-612.08914	-614.08591

^a ΔH_f° at 25 °C in hartree^b These molecules have also been calculated at the STO-3G, 3-21G, 6-31G* levels in Ref. [21]^c These molecules have been calculated at the HF/6-31G* and MP2(fc)/6-31G*//HF/6-31G* levels in Ref. [24]**Fig. 1.** The polycyclic aromatic hydrocarbons and the numbering system

electronic energies (hartree) for these methods are listed in Table 1 for several PAHs and for the compounds protonated at the positions indicated by the number. The numbering systems are shown for convenience in Fig. 1. The calculated proton affinities of benzene, naphthalene, anthracene, phenanthrene, biphenylene and fluoranthene with the different basis sets are listed in Table 2, along with the logarithm values of relative protodetrutiation rates [15, 18, 19] and experimental PA values [23].

For comparison purposes, calculations were also done with the semiempirical PM3 method. PM3 is parameterized to give ΔH_f° at 25°C. To obtain the PA values the ΔH_f° of H^+ was taken as the experimental value, 367.5 kcal mol⁻¹. As shown in Table 2, the values in column PM3 compare well with the experimental PA values, being low by an average of 2.8 kcal mol⁻¹ except for biphenylene.

**Fig. 2.** Rates of protodetrutiation compared to MP2/6-31G*//HF/6-31G* proton affinities. The *straight line* is based on the benzene, naphthalene, phenanthrene and anthracene (BNPA) points (*circles*), $-40.01 + 0.200x$, $R^2 = 0.953$. *Diamonds* are biphenylene; *squares* are fluoranthene

Some PA values have been determined previously using AM1 [22]. The ab initio results are not expected to reproduce the experimental PA results directly since the latter generally refer to temperatures about room temperature and the computed values pertain to 0 K. The MP2/6-31G*//HF/6-31G* calculations give values that are uniformly higher than experiment by 4.9 kcal mol⁻¹. Except for biphenylene, which deviates strongly from the trend of the other PAHs, the difference is 5.8 ± 1.7 kcal mol⁻¹. The 6-31G* results are higher than experiment by 17.8 ± 2.0 kcal mol⁻¹; biphenylene at this level is not markedly different from the other PAHs.

Table 2. The proton affinities of benzene, naphthalene, anthracene, phenanthrene, biphenylene, fluoranthene at different positions with several basis sets (kcal mol⁻¹)

Aromatic position	Symbol ^a	PM3 ^b	STO-3G	3-21G*	6-31G*	MP2	Log relative rate ^c	Exp. proton affinity ^d
Benzene	B	178.478	232.944	189.966	195.494	182.944	-3.00	179.3
Naphthalene-1	1N	190.096	250.941	205.208	210.398	198.161	(0)	191.9
Naphthalene-2	2N	186.799	246.053	200.596	206.626	193.775	-0.86	
Phenanthrene-1	1P	192.410	253.464	206.400	211.985	200.678	-0.03	
Phenanthrene-2	2P	189.767	249.705	203.194	209.733	197.515	-0.75	
Phenanthrene-3	3P	191.147	252.284	205.327	211.734	199.203	-0.40	
Phenanthrene-4	4P	189.730	251.832	205.516	211.282	200.408	-0.075	
Phenanthrene-9	9P	192.668	254.336	207.411	213.134	201.048	0.22	197.3
Anthracene-1	1A	196.198	260.492	213.052	218.442	205.886	0.76	
Anthracene-2	2A	192.240	255.177	208.346	214.771	201.217	0.00	
Anthracene-9	9A	204.482	273.544	225.050	229.361	217.307	4.17	209.7
Biphenylene-1	1Bi	186.669	246.856	199.090	206.601	193.794	-0.97	
Biphenylene-2	2Bi	191.449	257.304	209.820	218.185	203.407	1.16	202.7
Fluoranthene-1	1F	192.433	254.656	206.382	212.801	199.768	-0.52	
Fluoranthene-2	2F	188.846	248.406	201.431	207.875	195.770	-1.14	
Fluoranthene-3	3F	196.237	261.270	212.864	219.164	205.585	0.96	198.0
Fluoranthene-7	7F	192.083	251.901	204.694	210.693	201.211	-0.59	
Fluoranthene-8	8F	194.114	256.250	208.979	215.562	203.903	0.66	

^a Position numbers from Fig. 1^b Values are derived from heats of formation at 25°C using experimental $\Delta H_f^\circ(\text{H}^+) = 367.5$ kcal mol⁻¹ [23]^c Refs. [15, 18]^d Data are cited from Ref. [23]

The experimental PA results pertain to only the most reactive positions but protodetritiation rates are available for less reactive positions as well. The experimental rates correlate well with the MP2/6-31G**//HF/6-31G* values for simple alternant benzenoid systems, benzene, naphthalene, phenanthrene and anthracene (BNPA) (Fig. 2) as expected from the general correlation of such positions with all MO methods. Most important, however, is that the biphenylene and fluoranthene positions correlate almost as well as the “normal” positions; a linear regression based on all of the points, $-39.81 + 0.199x$ ($R^2 = 0.921$) is similar to the BNPA points alone. The largest deviation is for the fluoranthene 7-position which is 3.5 times less reactive than predicted by the BNPA correlation. This might reflect a steric hindrance effect at this position so that the rate of protonation does not in this case correlate with equilibrium protonation; however, the 4-position of phenanthrene with a similar steric situation correlates quite well and steric effects in protodetritiations are known to be small [25]. The order of reactivity of fluoranthene positions in nitration has been shown to be $3 > 8 > 7 > 1 > 2$ [14] in agreement with the calculated proton affinities; the difference from the order of protodetritiation reactivities is just a reversal of the 7- and 1-positions. The result may be an artifact of the basis set level; we note that the MP2 correction of the 6-31G* energies is greatest for the 7-position of all the protonated fluoranthenes.

The 6-31G* results give a correlation that is at least as good (Fig. 3). The biphenylene and fluoranthene points fit the BNPA correlation even better than the MP2 calculations and, in particular, the fluoranthene 7-position is no longer aberrant. A linear correlation based on all points is $-42.156 + 0.198x$ ($R^2 = 0.935$). Indeed, even the rather low level 3-21G* method does quite well as

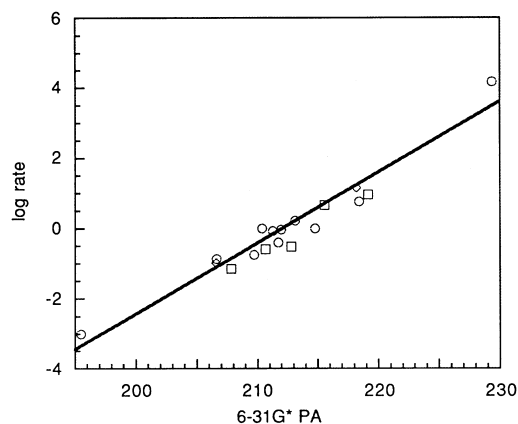
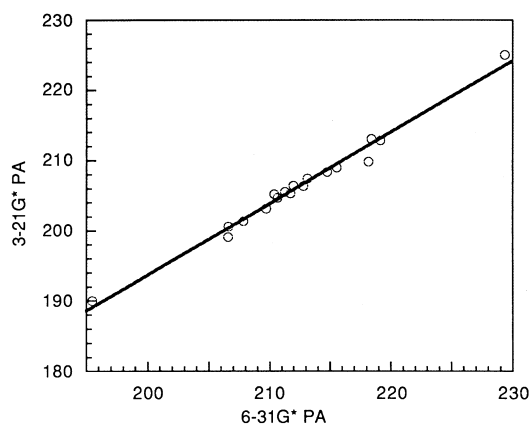
**Fig. 3.** Rates of protodetritiation compared to 6-31G*//HF/6-31G* proton affinities. The *straight line* is based on the BNPA points (*circles*), $-42.82 + 0.202x$, $R^2 = 0.947$. *Diamonds* are biphenylene; *squares* are fluoranthene**Fig. 4.** 3-21G* Proton affinities compared to 6-31G* values. The regression line is $-10.474 + 1.020x$, $R^2 = 0.985$

Table 3. Selected bond lengths and bond angles of neutral and protonated PAHs

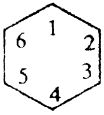
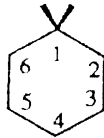
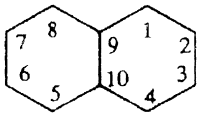
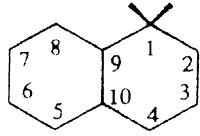
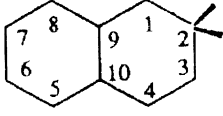
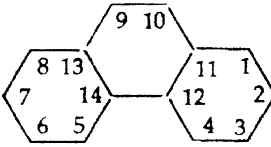
Molecule	Bond length, Å			Bond angle, degrees		
	Bond	Bond length	% change	Angle	Bond angle	% change
 Benzene	Cl—C2 ^{a,b}	1.387		C2—Cl—C6	120.000	
	Cl—H	1.076				
 B	Cl—C2	1.478	6.56	C2—Cl—C6	115.717	-3.57
	C2—C3	1.353	-2.45	C1—C2—C3	121.785	1.49
	C3—C4	1.410	1.66	C2—C3—C4	118.533	-1.22
	C1—H	1.094	1.67	C3—C4—C5	123.646	3.04
	C2—H	1.075	-0.09			
	C3—H	1.073	-0.28			
	C4—H	1.076	0.0			
 Naphthalene	C1—C2 ^{b,c}	1.358		C2—Cl—C9	120.775	
	C2—C3	1.417		C1—C2—C3	120.255	
	Cl—C9	1.421		C1—C9—C10	118.970	
	C9—C10	1.409				
	Cl—H	1.076				
	C2—H	1.075				
 1N	Cl—C2	1.483	9.20	C2—Cl—C9	115.706	-4.20
	C2—C3	1.349	-4.80	C1—C2—C3	123.003	2.29
	C3—C4	1.413	4.05	C2—C3—C4	118.746	-1.25
	C4—C10	1.400	-1.48	C3—C4—C10	123.925	2.61
	Cl—C9	1.500	5.56	C4—C10—C9	119.045	0.06
	C9—C10	1.416	0.50	C1—C9—C10	119.574	0.51
	Cl—H	1.090	1.30			
	C2—H	1.075	0.0			
	C3—H	1.073	-0.19			
	C4—H	1.076	0.0			
 2N	Cl—C2	1.477	8.76	C2—Cl—C9	123.079	1.91
	C2—C3	1.488	5.01	C1—C2—C3	114.967	-4.40
	C3—C4	1.331	-1.99	C2—C3—C4	122.040	1.48
	C4—C10	1.449	1.97	C3—C4—C10	120.950	0.14
	Cl—C9	1.362	-4.15	C4—C10—C9	119.993	0.86
	C9—C10	1.441	2.27	C1—C9—C10	118.970	0.0
	Cl—H	1.076	0.0			
	C2—H	1.092	1.58			
	C3—H	1.074	-0.09			
	C4—H	1.074	-0.19			
 Phenanthrene	Cl—C2 ^{b,d}	1.366		C2—Cl—C11	121.014	
	C2—C3 ^e	1.402		C1—C2—C3	119.470	
	C3—C4	1.368		C2—C3—C4	120.386	
	C4—C12	1.411		C3—C4—C12	121.370	
	C1—C11	1.409		C1—C11—C12	119.837	
	C11—C12	1.404		C4—C12—C11	117.924	
	C10—C11	1.441		C9—C10—C11	121.098	
	C9—C10	1.339		C10—C11—C12	119.811	
	C12—C14	1.461		C11—C12—C14	119.091	
	C1—H	1.076				
	C2—H	1.075				
	C3—H	1.075				
	C4—H	1.072				
	C9—H	1.076				

Table 3 (Contd.)

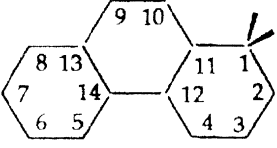
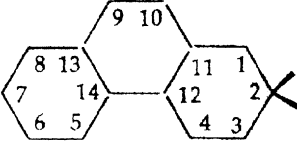
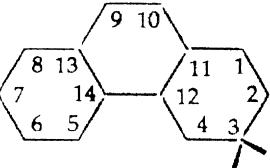
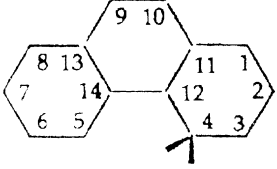
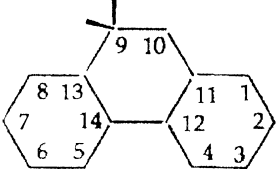
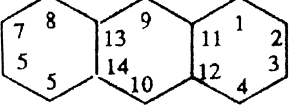
Molecule	Bond length, Å			Bond angle, degrees			
	Bond	Bond length	% change	Angle	Bond angle	% change	
 <p>1P</p>	C1—C2	1.482	8.49	C2—C1—C11	116.262	-3.93	
	C2—C3	1.340	-4.42	C1—C2—C3	121.670	1.84	
	C3—C4	1.425	4.17	C2—C3—C4	119.266	-0.93	
	C4—C12	1.387	-1.70	C3—C4—C12	124.921	2.93	
	C1—C11	1.498	6.32	C1—C11—C12	120.511	0.56	
	C11—C12	1.416	0.85	C4—C12—C11	117.370	-0.47	
	C1—H	1.090	1.30				
	C2—H	1.075	0.0				
	C3—H	1.073	-0.19				
	C4—H	1.073	0.09				
	 <p>2P</p>	C1—C2	1.476	8.05	C2—C1—C11	123.769	2.28
		C2—C3	1.482	5.71	C1—C2—C3	114.126	-4.47
		C3—C4	1.334	-2.49	C2—C3—C4	122.396	1.67
C4—C12		1.448	2.62	C3—C4—C12	121.532	0.13	
C1—C11		1.354	-3.90	C1—C11—C12	119.426	-0.34	
C11—C12		1.445	2.92	C4—C12—C11	118.752	0.70	
C1—H		1.076	0.0				
C2—H		1.092	1.58				
C3—H		1.075	0.0				
C4—H		1.069	-0.28				
 <p>3P</p>		C1—C2	1.332	-2.49	C2—C1—C11	121.186	0.14
		C2—C3	1.484	5.85	C1—C2—C3	121.489	1.69
		C3—C4	1.481	8.26	C2—C3—C4	114.917	-4.54
	C4—C12	1.353	-4.11	C3—C4—C12	124.228	2.35	
	C1—C11	1.446	2.63	C1—C11—C12	120.698	0.72	
	C11—C12	1.448	3.13	C4—C12—C11	117.482	-0.37	
	C1—H	1.074	-0.19				
	C2—H	1.075	0.0				
	C3—H	1.092	1.58				
	C4—H	1.073	0.09				
	 <p>4P</p>	C1—C2	1.419	3.88	C2—C1—C11	124.511	2.89
		C2—C3	1.342	-4.28	C1—C2—C3	118.355	-0.93
		C3—C4	1.484	8.48	C2—C3—C4	122.510	1.76
C4—C12		1.500	6.31	C3—C4—C12	116.508	-4.01	
C1—C11		1.392	-1.21	C1—C11—C12	119.160	-0.56	
C11—C12		1.408	0.28	C4—C12—C11	118.956	0.88	
C1—H		1.076	0.0				
C2—H		1.073	-0.19				
C3—H		1.075	0.0				
C4—H		1.090	1.68				
 <p>9P</p>		C9—C10	1.472	9.93	C9—C10—C11	123.838	2.26
		C10—C11	1.360	-5.62	C10—C11—C12	119.895	0.07
		C11—C12	1.445	2.92	C11—C12—C14	120.123	0.87
	C12—C14	1.462	0.07	C12—C14—C13	119.704	0.51	
	C9—C13	1.501	4.16	C10—C9—C13	115.352	-4.74	
	C13—C14	1.400	-0.28	C9—C13—C14	121.087	1.07	
	C9—H	1.091	1.39				
	C10—H	1.076	0.0				
	 <p>Anthracene</p>	C1—C2 ^{b,d}	1.348		C2—C1—C11	120.904	
		C2—C3 ^f	1.433		C1—C2—C3	120.485	
C1—C11		1.436		C1—C11—C12	118.611		
C11—C12		1.425		C9—C11—C12	119.241		
C9—C11		1.389		C11—C9—C13	121.517		
C1—H		1.076					
C2—H		1.075					
C9—H		1.077					

Table 3 (Contd.)

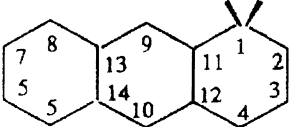
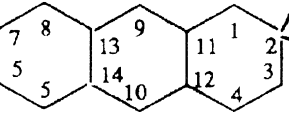
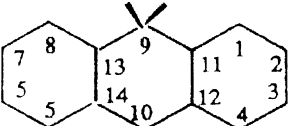
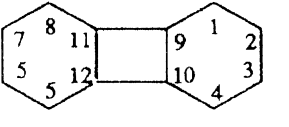
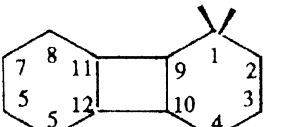
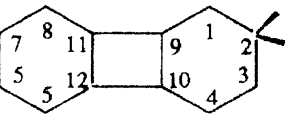
Molecule	Bond length, Å			Bond angle, degrees			
	Bond	Bond length	% change	Angle	Bond angle	% change	
 1A	C1—C2	1.489	10.46	C2—C1—C11	115.244	-4.68	
	C2—C3	1.346	-6.07	C1—C2—C3	123.707	2.67	
	C3—C4	1.419	5.27	C2—C3—C4	118.995	-1.24	
	C4—C12	1.391	-3.13	C3—C4—C12	123.427	2.09	
	C1—C11	1.508	5.01	C1—C11—C12	118.813	0.17	
	C11—C12	1.440	1.05	C4—C12—C11	119.814	1.01	
	C1—H	1.089	1.21				
	C2—H	1.076	0.09				
	C3—H	1.073	-0.19				
	C4—H	1.076	0.0				
	 2A	C1—C2	1.481	9.87	C2—C1—C11	123.023	1.75
		C2—C3	1.496	4.40	C1—C2—C3	114.398	-5.05
		C3—C4	1.326	-1.63	C2—C3—C4	122.557	1.72
C4—C12		1.460	1.67	C3—C4—C12	121.614	0.59	
C1—C11		1.359	-5.36	C1—C11—C12	120.109	1.26	
C11—C12		1.454	2.04	C4—C12—C11	118.299	-0.26	
C1—H		1.077	0.09				
C2—H		1.091	1.49				
C3—H		1.074	-0.09				
C4—H		1.074	-0.19				
 9A		C9—C11	1.504	8.28	C9—C11—C12	120.547	1.10
		C11—C12	1.412	-0.91	C10—C12—C11	119.202	-0.03
		C10—C12	1.404	1.08	C12—C10—C14	124.386	2.36
	C9—H	1.088	1.02	C11—C9—C13	116.114	-4.45	
	C10—H	1.077	0.0				
	 Biphenylene	C1—C2	1.418		C2—C1—C9	115.698	
		C2—C3	1.373		C1—C2—C3	121.866	
C1—C9		1.356		C1—C9—C10	122.436		
C9—C10		1.414		C10—C9—C11	90.000		
C9—C11		1.507					
C1—H		1.075					
C2—H		1.075					
 1Bi		C1—C2	1.509	6.42	C2—C1—C9	110.873	-4.17
	C2—C3	1.332	-2.99	C1—C2—C3	123.485	1.33	
	C3—C4	1.469	3.60	C2—C3—C4	122.466	0.49	
	C4—C10	1.337	-1.40	C3—C4—C10	117.511	1.57	
	C1—C9	1.471	8.48	C1—C9—C10	123.340	0.74	
	C9—C10	1.428	0.99	C4—C10—C9	122.324	-0.09	
	C9—C11	1.434	-4.84	C10—C9—C11	92.195	2.44	
	C1—H	1.091	1.49	C9—C10—C12	87.363	-2.93	
	C2—H	1.074	-0.09				
	C3—H	1.073	-0.19				
	C4—H	1.074	-0.09				
	 2Bi	C1—C2	1.504	6.06	C2—C1—C9	116.928	1.06
		C2—C3	1.499	9.18	C1—C2—C3	116.125	-4.71
C3—C4		1.356	-4.37	C2—C3—C4	125.719	3.16	
C4—C10		1.403	3.47	C3—C4—C10	114.156	-1.33	
C1—C9		1.319	-2.73	C1—C9—C10	123.380	0.77	
C9—C10		1.459	3.18	C4—C10—C9	123.690	1.02	
C9—C11		1.499	-0.53	C10—C9—C11	87.006	-3.33	
C1—H		1.074	-0.09	C9—C10—C12	91.041	1.16	
C2—H		1.090	1.40				
C3—H		1.076	0.09				
C4—H		1.073	-0.19				

Table 3 (Contd.)

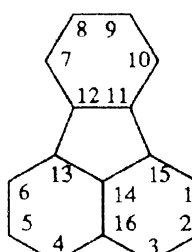
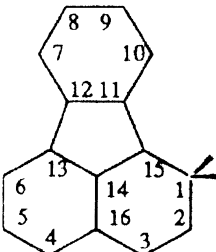
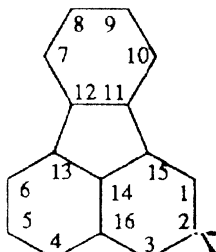
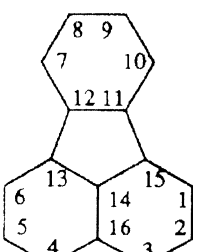
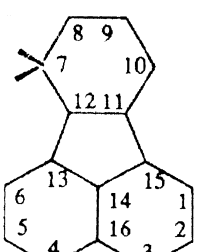
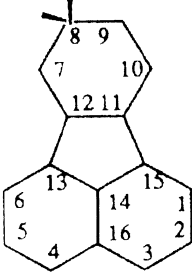
Molecule	Bond length, Å			Bond angle, degrees			
	Bond	Bond length	% change	Angle	Bond angle	% change	
 Fluoranthene	C1—C15	1.360		C14—C15—C1	118.589		
	C1—C2	1.424		C15—C1—C2	118.557		
	C2—C3	1.365		C1—C2—C3	122.450		
	C3—C16	1.423		C2—C3—C16	120.023		
	C1—C15	1.413		C15—C14—C16	124.215		
	C15—C14	1.383		C3—C16—C14	116.166		
	C11—C15	1.481		C13—C14—C15	111.569		
	C11—C12	1.411		C11—C15—C14	106.010		
	C7—C12	1.379		C15—C11—C12	108.206		
	C7—C8	1.391		C7—C12—C11	120.380		
	C8—C9	1.385		C12—C7—C8	118.922		
	C1—H	1.076		C7—C8—C9	120.697		
	C2—H	1.076					
	C3—H	1.076					
C7—H	1.076						
C12—H	1.075						
 1F	C1—C15	1.481	8.90	C14—C15—C1	119.825	1.04	
	C1—C2	1.504	5.62	C15—C1—C2	113.615	-4.17	
	C2—C3	1.333	-2.34	C1—C2—C3	124.184	1.42	
	C3—C16	1.456	2.32	C2—C3—C16	120.294	0.23	
	C1—C15	1.385	-1.98	C15—C14—C16	124.381	0.13	
	C15—C14	1.395	0.87	C3—C16—C14	117.700	1.32	
	C11—C15	1.452	-1.96	C11—C15—C14	108.168	2.04	
	C14—C13	1.419	0.42	C13—C14—C15	110.960	-0.55	
	C1—H	1.091	1.39	C15—C11—12	107.823	-0.35	
	C2—H	1.075	-0.09				
	C3—H	1.074	-0.19				
	 2F	C1—C15	1.335	-1.84	C14—C15—C1	118.392	-0.17
		C1—C2	1.497	5.13	C15—C1—C2	120.331	1.50
		C2—C3	1.486	8.86	C1—C2—C3	117.187	-4.30
C3—C16		1.363	-4.22	C2—C3—C16	122.267	1.87	
C1—C15		1.441	1.98	C15—C14—C16	125.827	1.30	
C15—C14		1.413	2.17	C3—C16—C14	115.996	-0.15	
C11—C15		1.481	0.0	C11—C15—C14	105.541	-0.44	
C14—C13		1.394	-1.34	C1—C15—C8	110.874	-0.62	
C1—H		1.075	-0.09	C1—C14—C9	108.408	0.19	
C2—H		1.077	1.58				
C3—H		1.093	0.09				
 3F		C1—C15	1.418	4.26	C14—C15—C1	120.146	1.31
		C1—C2	1.351	-5.13	C15—C1—C2	117.544	-0.85
		C2—C3	1.497	9.67	C1—C2—C3	125.548	2.53
	C3—C16	1.499	5.34	C2—C3—C16	114.745	-4.40	
	C1—C15	1.427	0.99	C15—C14—C16	124.676	0.37	
	C15—C14	1.372	-0.80	C3—C16—C14	117.341	1.01	
	C11—C15	1.442	-2.63	C11—C15—C14	107.318	1.23	
	C14—C13	1.404	-0.64	C1—C15—C8	110.565	-0.90	
	C1—H	1.073	-0.28	C1—C14—C9	110.310	-0.91	
	C2—H	1.076	0.0				
	C3—H	1.090	1.30				
	 7F	C7—C12	1.484	7.61	C12—C7—C8	114.335	-3.86
		C7—C8	1.493	7.33	C7—C8—C9	122.514	1.51
		C8—C9	1.336	-3.54	C8—C9—C10	120.221	-0.39
C9—C10		1.442	3.67	C9—C10—C11	122.169	2.73	
C10—C11		1.363	-1.16	C7—C12—C11	121.264	0.73	
C11—C12		1.422	0.78	C10—C11—C12	119.496	-0.73	
C12—C13		1.421	-4.05	C11—C12—C13	108.917	0.66	
C11—C15		1.476	-0.34	C12—C11—C15	107.842	-0.34	
C7—H		1.091	1.39				
C8—H		1.074	-0.09				
C9—H		1.073	-0.19				
C10—H		1.076	0.0				

Table 3 (Contd.)

Molecule	Bond length, Å			Bond angle, degrees		
	Bond	Bond length	%change	Angle	Bond angle	%change
 8F	C7—C12	1.336	-3.12	C12—C7—C8	121.304	2.00
	C7—C8	1.489	7.05	C7—C8—C9	115.518	-4.29
	C8—C9	1.488	7.44	C8—C9—C10	123.199	2.07
	C9—C10	1.342	-3.52	C9—C10—C11	118.474	-0.38
	C10—C11	1.425	3.34	C7—C12—C11	119.830	-0.46
	C11—C12	1.460	3.47	C10—C11—C12	121.675	1.08
	C12—C13	1.479	-0.14	C11—C12—C13	107.075	-1.05
	C11—C15	1.419	-4.19	C12—C11—C15	108.349	0.13
	C7—H	1.075	-0.09			
	C8—H	1.091	1.49			
	C9—H	1.075	0.0			
	C10—H	1.073	-0.28			

^a Experimental bond lengths: Ref. [26]

^b Experimental bond lengths: Ref. [27]

^c Experimental bond lengths: Ref. [28]

^d Experimental bond lengths: Ref. [29]

^e Bond lengths of neutral phenanthrene have also been calculated at the HF/STO-3G level: Ref. [30]

^f Experimental results: Ref. [31]

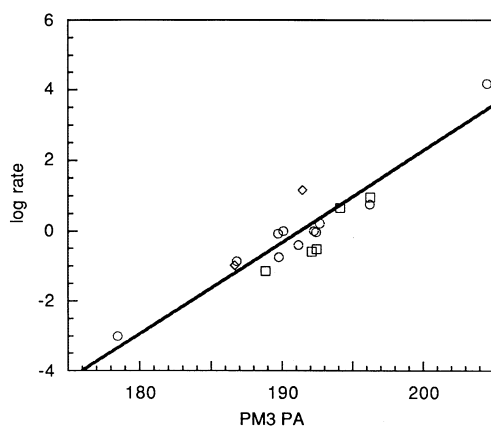


Fig. 5. Rates of protodetrithiation compared to PM3 proton affinities. The straight line is based on the BNPA points (circles), $-49.99 + 0.261x$, $R^2 = 0.942$. Diamonds are biphenylene; squares are fluoranthene

indicated by comparison of 3-21G* and 6-31G* proton affinities in Fig. 4. Correspondingly, correlation of the logarithm of the relative rates for protodetrithiation with 3-21G* proton affinities gives a regression of $-40.52 + 0.196x$ ($R^2 = 0.967$) for the BNPA points and $-40.03 + 0.194x$ ($R^2 = 0.945$) for all the points.

The lowest ab initio level, STO-3G, gives a good correlation for the BNPA positions ($-42.657 + 0.169x$; $R^2 = 0.952$) but does significantly more poorly when biphenylene and fluoranthene points are included ($-42.547 + 0.168x$; $R^2 = 0.922$). The semiempirical PM3 method also gives a good correlation for most of the positions (Fig. 5). The point farthest off the regression line based on BNPA is 2-biphenylene.

In all these correlations with protodetrithiation rates, the 9-position of anthracene (9A) is more reactive than predicted from its calculated equilibrium proton affinity.

It is also by far the most reactive position in this series. This might indicate a significant change in transition structure. We also sought changes in molecular structure on protonation. Table 3 summarizes structural data at the 6-31G* level for the protonated ring of these PAHs and lists the percentage changes from the neutral hydrocarbon.

When protonation takes place, the two C—C bonds connected to the protonated position are longer because these bonds are now $C_{sp^2}-C_{sp^3}$. Of the compounds examined here, only at the anthracene 9-position are both bonds connected to a ring junction. The uniqueness of such positions has been cited previously [22]. Thus, as shown in Table 3, the total percentage change of the two C—C bonds connected to the protonated position in 9A is 16.56%, the largest number among these protonated molecules.

We conclude that calculations at any of these levels should provide excellent predictions of electrophilic aromatic substitution, particularly for normal benzenoid hydrocarbons. The best correlations are given by the HF/6-31G* method. MP2 correction at the 6-31* geometries gives slightly poorer agreement.

Acknowledgements. This work was supported in part by NSF grant CHE 95-28273. Dedicated to the memory of Kenichi Fukui whose earliest work included a theoretical study of aromatic substitution.

References

- Santodonato J, Howard P, Basu D (1981) In: Lee SD, Grant L (eds) Health and ecological assessment of polynuclear aromatic hydrocarbons. Pathotox, Park Forest S., Ill. p 177
- Cooke M, Dennis AJ (eds) (1986) Polynuclear aromatic hydrocarbons: chemistry, characterization and carcinogenesis. Battelle Press, Columbus, Ohio

3. Jones PW, Leber P (1979) Polynuclear aromatic hydrocarbons; 3rd international symposium on chemistry and biology-carcinogenesis and mutagenesis. Ann Arbor Science Publishers, Ann Arbor, Mich
4. Laali KK (1996) Chem Rev 96:1873
5. Cavalieri EL, Rogan EG (1985) In: Harvey RG (ed) Polycyclic hydrocarbons and carcinogenesis, ACS symposium series 283. American Chemical Society, Washington, D. C., pp 289
6. Ramakrishna NVS, Cavalieri EL, Rogan EG, Dolnokowski G, Cerny RL, Gross ML, Jeong H, Jankowiak R, Small GJ (1992) J Am Chem Soc 114:1863
7. Rogan EL, Devarasan PD, Cavalieri EL (1991) In: Cook M, Leoning L, Merritt J (eds) Polynuclear aromatic hydrocarbons: measurements, means, and metabolism. Battelle Press, Columbus, Ohio, p 767
8. Streitwieser A Jr (1961) Molecular orbital theory for organic chemists. Wiley, New York
9. Fukui K, Yonezawa T, Shingu H (1952) J Chem Phys 20:722
10. Fukui K, Yonezawa T, Nagata C, Shingu H (1954) J Chem Phys 22:1433
11. Dewar MJS (1952) J Am Chem Soc 74:3357
12. Dewar MJS, Mole T, Warford EWT (1956) J Chem Soc:3581
13. Dewar MJS (1958) Rec Chem Prog 19:1
14. Streitwieser A Jr, Fahey RC (1962) J Org Chem 27:2352
15. Bancroft KCC, Howe GR (1970) J Chem Soc B:1541
16. Streitwieser A Jr, Mowery PC, Jesaitis RG, Lewis A (1970) J Am Chem Soc 92:6529
17. Lias SG, Bartmess JE, Liebman JF, Holmes JL, Levin RD, Mallard WG (1988) J Phys Chem Ref Data 17, Suppl no. 1:1
18. Streitwieser A Jr, Lewis A, Schwager I, Fish RW, Labana S (1970) J Am Chem Soc 92:6525
19. Bancroft KCC, Bott RW, Eaborn C (1972) J Chem Soc Perkin Trans II:95
20. (a) G Frisch MJ, Trucks GW, Schlegel HB, Gill PMW, Johnson BG, Wong MW, Foresman JB, Robb MA, Head-Gordon M, Replogle ES, Gomperts R, Andres JL, Raghavachari K, Binkley JS, Gonzalez C, Martin RL, Fox DJ, Defrees DJ, Baker J, Stewart JJP, Pople JA (1993) Gaussian 92/DFT, revision G.1. Gaussian, Pittsburgh, Pa; (b) Frisch MJ, Trucks GW, Schlegel HB, Gill PMW, Johnson BG, Robb MA, Cheeseman JR, Keith T, Petersson GA, Montgomery JA, Raghavachari K, Al-Laham MA, Zakrzewski VG, Ortiz JV, Foresman JB, Cioslowski J, Stefanov BB, Nanayakkara A, Challacombe M, Peng CY, Ayala PY, Chen W, Wong NW, Andres JL, Replogle ES, Gomperts R, Martin RL, Fox DJ, Binkley JS, Defrees DJ, Baker J, Stewart JP, Head-Gordon M, Gonzalez C, Pople JA (1995) Gaussian 94, revision C3. Gaussian, Pittsburgh, Pa
21. Schulman MJ, Peck RC, Disch RL (1989) J Am Chem Soc 111:5675
22. Pointet K, Milliet A, Hoyan S, Renou-Gonnord MF (1997) J Comput Chem 18:629
23. Hunter EP, Lias SG (1998) J Phys Chem Ref Data (in press). See <http://webbook.nist.gov/chemistry/>
24. Eckert-Maksic M, Fabian WMF, Janoschek R, Maksic ZB (1995) J Mol Struct (Theochem) 338:1
25. Baker R, Eaborn C, Taylor R (1961) J Chem Soc:4927
26. Tamagawa K, Lijima T, Kimura M (1976) J Mol Struct 30:243
27. Kao J, Allinger NL (1977) J Am Chem Soc 99:975
28. Bastiansen Q, Shancke PN (1961) Adv Chem Phys 3:323
29. Kay MI, Okaya Y, Lox DE (1971) Acta Crystallogr Sect B 27:26
30. Schulman JM, Peck RC, Disch RL (1989) J Am Chem Soc 111:5675
31. Mason R (1964) Acta Crystallogr 17:547